AJNR

Quantitative sonographic feature analysis of clinical infant hypoxia: a pilot study.

L L Barr, P J McCullough, W S Ball, Jr, B H Krasner, B S Garra and J A Deddens

AJNR Am J Neuroradiol 1996, 17 (6) 1025-1031
http://www.ajnr.org/content/17/6/1025

Quantitative Sonographic Feature Analysis of Clinical Infant Hypoxia: A Pilot Study

Lori L. Barr, Patrick J. McCullough, William S. Ball, Jr, Brian H. Krasner, Brian S. Garra, and James A. Deddens

PURPOSE: To determine whether textural features derived from sonographic pixel intensities differ significantly between healthy infants and infants who have had acute clinical hypoxic episodes. **METHODS:** Neurosonographic and calibration phantom–processed image data were evaluated prospectively from 9 infants (age range, 1 to 163 days) with at least 1 episode of hypoxia and compared with image data from a control population of 16 healthy infants (age range, 1 to 191 days). Custom software was used to make 45 textural feature measurements on 40 × 40-pixel regions of interest within brain parenchyma in the distribution of each major cerebral artery, the thalami, and the cerebellum and in a tissue-mimicking calibration phantom. Means comparison testing was followed by logistic regression to assess statistical variation between the patients and the control group. **RESULTS:** Nine of 45 textural features showed statistically significant differences between mean values comparing the two groups. Mean gray level was the most sensitive predictor of differences between the two populations (mean gray level for healthy subjects was 46.8; mean gray level for patients was 56.3). An average of mean gray values in areas supplied by the posterior cerebral arteries and the cerebellum was even more sensitive for differentiating healthy subjects from patients. **CONCLUSIONS:** Quantitative sonographic textural feature analysis showed differences between the brains of healthy infants and those of infants with clinical hypoxia.

Index terms: Brain, ultrasound; Hypoxia; Infants, injuries

AJNR Am J Neuroradiol 17:1025–1031, June 1996

Sonography is a commonly used technique for the initial and follow-up examination of infants with a clinical history or physical findings of hypoxia (1). While the qualitative approach to sonographic interpretation currently used is very good at distinguishing focal areas of abnormal echogenicity from infarction or hemorrhage, interpretation becomes more difficult when the pathologic process is subtle or alters the image texture in a more diffuse pattern, such as may be found with cerebral edema or hypoxic/ischemic encephalopathy. Previous investigators (2) have demonstrated that increased echogenicity, convolutional effacement, and obliteration of extraaxial fluid spaces around the brain can be reliable indicators of hypoxic/ischemic encephalopathy on neurosonograms (Fig 1). However, as many as 50% of neurosonograms in such cases show normal echogenicity on gray-scale images (Fig 2) (1). Methods of quantitatively measuring sonographic image data have been useful in identifying diffuse diseases of the liver (3–5). A general term for this process is *textural feature analysis* (6). The purpose of our study was to determine whether textural features derived from sonographic image pixel intensities differed significantly between healthy infants and infants with clinical hypoxia, and to determine whether such textural feature analysis can improve detection of clinical sequelae of brain injury.

Received November 7, 1994; accepted after revision January 16, 1996.

Funded in part by a grant from the RSNA Research and Education Fund and the Department of Radiology at Children's Hospital Medical Center.

From the Department of Radiology, Children's Hospital Medical Center, Cincinnati, Ohio (L.L.B., P.J.M., W.S.B.); the Departments of Imaging Physics (B.H.K.) and Radiology (B.S.G.), Georgetown University Hospital, Washington, DC; and the Department of Mathematical Science, University of Cincinnati, Ohio (J.A.D.).

Address reprint requests to: Lori L. Barr, MD, Department of Radiology, Children's Hospital Medical Center, 3333 Burnet Ave, Cincinnati, OH 45229.

AJNR 17:1025–1031, Jun 1996 0195-6108/96/1706–1025

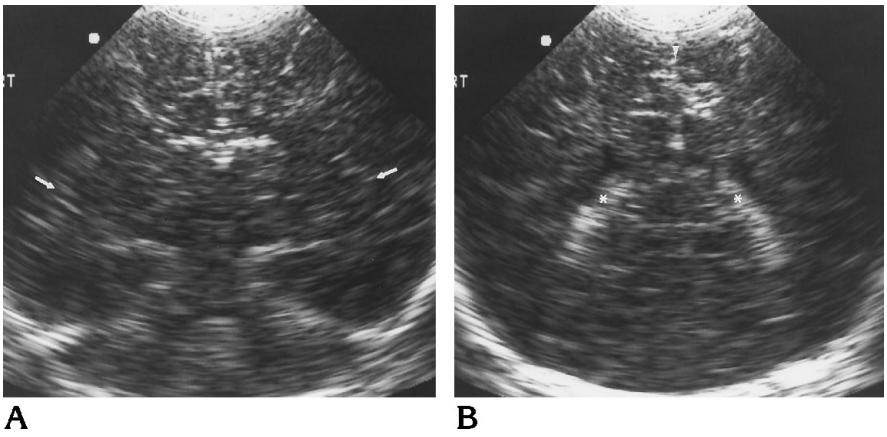

Fig 1. Coronal neurosonograms performed 4 days after birth of an infant with an Apgar score of 0/4 at 1 and 5 minutes after emergency cesarean section for fetal decelerations.

A, Note obliteration of the extraaxial fluid spaces and the ventricle as evidenced by the lack of definition of the sylvian fissures (*arrows*). The overall echogenicity of the brain is normal, although the echoes are coarse in all areas seen. The patient's mean gray level was 57.71.

B, Image obtained through the parietooccipital region shows virtually no fluid around the choroid plexus (*asterisks*) in the lateral ventricles. No fluid is seen adjacent to the falx (*arrowhead*). Generalized coarseness of the echotexture is noted. The patient's combined mean gray level for the cerebellum and right and left posterior cerebral artery distributions was 59.54.

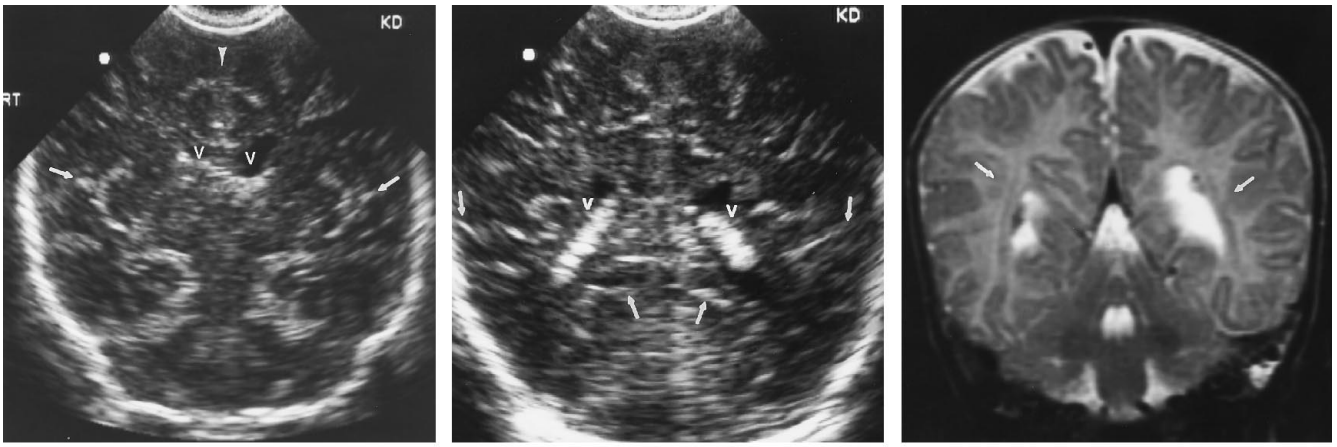

Fig 2. This 18-day-old infant had new onset of focal seizures and an acute hypoxic episode at 11 days of age.

A, Coronal neurosonogram through the region of the sylvian fissures shows normal echogenicity and echotexture. Note that the convolutional markings are easily delineated in the region of the falx (*arrowhead*) and the sylvian fissures (*arrows*). The anterior horns of the lateral ventricles (*V*) are normal in size, and asymmetry is a normal variant. This patient's overall mean gray level was 57.75.

B, Coronal neurosonogram through the occipital lobes shows normal echogenicity and normal convolutional markings (*arrows*). The lateral ventricles (*V*) are normal. The combined mean gray level (cerebellum and right and left posterior cerebral artery distribution) was 56.36.

C, Coronal fast spin-echo magnetic resonance image (2500/119 [repetition time/echo time]) obtained 9 months later shows white matter loss. Note decrease in the thickness of the periventricular white matter of the occipital lobes adjacent to the lateral ventricles (*arrows*).

Subjects and Methods

Neurosonograms were obtained prospectively in 9 infants (age range, 1 to 163 days) with a documented hypoxic episode and in a control group of 16 healthy infants (age range, 3 to 191 days). Hypoxia was defined as frank cyanosis lasting for more than 1 minute or asphyxia. Because this was a pilot study, the inclusion criteria were broad: low Apgar scores consistent with asphyxia (<5 at 1 minute, <5 at 5 minutes) or cardiopulmonary arrest after birth (n = 5); new onset of seizures associated with a clinical hypoxic episode (n = 2); or an acute hypoxic episode superimposed on chronic lung disease (n = 2). The ages of the patients and the timing of the sonograms after injury are shown in Figure 3.

The sonographic equipment (ATL Ultramark 9, Advanced Technology Laboratories, Bothell, Wash) was optimized before imaging of each patient. This involved altering 17 of 46 different scanning parameters including power, gain settings, image depth, focal zone location, and choice of two different mechanical sector transducers so that the sonographer was satisfied that the entire brain was best seen in both coronal and sagittal scan planes. The

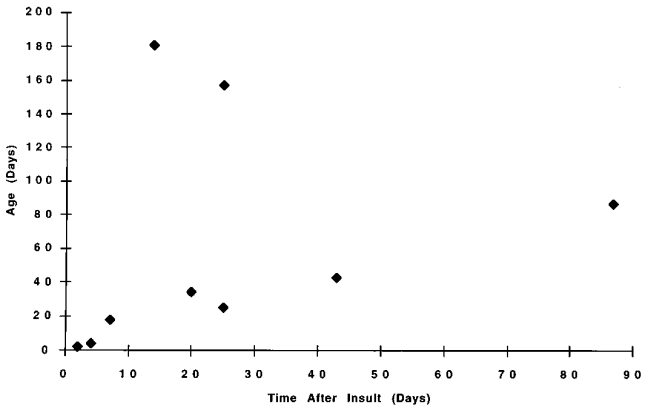

Fig 3. Ages of patients versus timing of sonographic examination after insult.

TABLE 1: Scanning parameters for patient and control groups

	Patients (n = 9)	Control Subjects (n = 16)
Scan depth, cm	7.9–11.0	9.8–12.6
Frequency, MHz	5.0	7.5–3.0
Power (%)	25.12–100	15.85–100
Time gain curve 1*	19	19–26
Time gain curve 2*	0	0–1040
Time gain curve 3*	27	27–80
Degree of frame averaging	3, 4	3, 4
Scanhead port	1, 2	1, 2
Frame rate, lines per second	980–1299	882–1495
Scanhead model*	32, 65	32, 33, 65
Time gain curve slide pot 1*	110–185	93–189
Time gain curve slide pot 2*	153–224	151–213
Time gain curve slide pot 3*	174–255	173–236
Time gain curve slide pot 4*	191–255	182–255
Time gain curve slide pot 5*	200–255	196–255
Time gain curve slide pot 6*	205–255	210–255
Time gain curve slide pot 7*	210–255	211–255
Time gain curve slide pot 8*	198–255	187–255

* Arbitrary values.

range of scanning parameters used in both populations is listed in Table 1. No attempt was made to limit the sonographer's or the machine's capacity to render the best images possible for each infant studied. A tissue-mimicking calibration phantom (RMI 403, Gammex RMI, Middleton, Wis) was imaged in the coronal and sagittal planes to capture a homogeneous sample of the effects of the machine settings. The phantom was scanned in the sagittal and coronal planes with 24 machine settings held constant during acquisition of the patient's and the phantom's sonograms. The sonographic unit was modified to download stored image data into a Macintosh IIfx personal computer (Apple Computer, Cupertino, Calif) for scan conversion. The 8-bit image data were then transferred to a Sun Sparcstation 2 (Sun Microsystems Inc, Mountain View, Calif) for analysis with the use of customized tissue-signature software (6).

The customized software allows image visualization, region of interest (ROI) sizing and positioning, and calculation of 45 textural features. These features are first-order and second-order gray-level statistics derived from the pixel intensities within the selected ROIs. First-order gray-level statistics describe the occurrence frequency of the gray levels, regardless of location or spatial interdependency. The gray-level histogram allows calculation of mean gray level, the upper and lower 10th percentile ranges for gray levels, gray-level variance, and skewness (deviation from symmetry). The second-order gray-level statistics describe the relationship between each pixel in the ROI and its neighboring pixels. These include gradient distribution analysis, co-occurrence matrix analysis, run-length histographic analysis, and fractal features analysis (4, 6).

Gradient analysis measures the intensity difference between each pixel and all neighboring pixels in order to identify directional trends in gray levels. The gradient is calculated by defining a rectangular neighborhood for each pixel and then calculating the absolute value and direction of the local gray-level difference gradient. Mean gradient absolute value, gradient value variance, and relative frequency of the most dominant edge with respect to the number of gradient elements in the ROI may then be calculated (3).

The gray level co-occurrence matrix is a two-dimensional histogram that characterizes the occurrence of gray levels in spatially related pixel pairs that may be closely related (two pixels) or farther apart (four pixels). Analysis involves the search for a pattern of intensity variation between a pixel and its neighbors in several different directions (north to south, east to west, and southwest to northeast). The features extracted include contrast, which measures how many large gray-level differences there are in the ROI; angular second moment, which measures the degree of clustering about major gray-level transitions; entropy, which measures uniformity of matrix values; and correlation, which measures the linearity of the relationship of the spatially related pixels (3).

Run-length histographic analysis counts the number of gray-level runs by their length and gray-level ranges. It quantifies the homogeneity of the ROI. A run is a set of vertically or horizontally neighboring pixels displaying similar levels of gray. We typically use lengths of two and four pixels. Parameters include run percentages in the horizontal and vertical directions, which characterize the distribution of runs; and long-run emphasis in the horizontal and vertical directions, which describes the frequency of occurrence of long runs (3, 4).

Fractal features analysis involves calculation of the fractional dimension of the irregular surfaces created when the pixel intensities are displayed as a histogram. Mandelbrot (7) defined fractals as objects that are heterogeneous, self-similar, and impossible to measure with a single unit of measure. While perfect fractal surfaces have a constant dimension over all ranges of scales, gray-level images are imperfect fractal surfaces and thus demonstrate a constant dimension over only those scales that reflect the size of the

TABLE 2: Clinical course of patient group

Patient	Initial Clinical Condition	Condition at 2-Year Follow-up
1	Acute respiratory arrest	Severe spastic quadriparesis/ developmental delay
2	Neonatal asphyxia	Death (anoxic encephalopathy)
3	Neonatal asphyxia	Mineralizing vasculopathy global white matter loss
4	Seizures, fever and diarrhea, acute hypoxic episode	Global cortical loss
5	Neonatal asphyxia	Anoxic encephalopathy, mild developmental delay
6	Seizures, acute hypoxic episode	Thalamic infarctions and global white matter loss, periventricular gliosis
7	Acute respiratory arrest	Global cognative and motor developmental delay
8	Acute status epilepticus with cardiopulmonary arrest	Global supratentorial/ infratentorial parenchymal loss, spastic quadriparesis, cortical blindness
9	Neonatal asphyxia	Mild developmental delay

anatomic structures of interest (5). We thus tested several different scale ranges to measure the fractal dimension of the surface created by the varying pixel intensities within the ROI.

In each patient, four to six 40 × 40-pixel ROIs were positioned in the anterior, middle, and posterior cerebral artery distributions bilaterally; in both thalami; in the cerebellum; and on the images of the tissue-mimicking calibration phantom. The textural feature data included repeated measurements of varying number in each infant. Therefore, we chose univariate analysis using the method of generalized estimating equations (GEE) as described by Zeger and Liang (8). This method takes into account the correlation between the observations for each individual and (in contrast to the usual repeated measures analysis) allows for varying numbers of observations per subject.

An average value for each textural feature at each anatomic location for each infant was computed. Then, logistic regression was used to find the best combination of features and/or locations for predicting that a given infant would have brain abnormalities (9). *P* values were determined by the likelihood ratio test (9).

The subjects were followed up for a period of 2 years to assure that the group of patients had documented evidence of hypoxic sequelae. These findings are summarized in Table 2.

Results

Means comparison testing of the external tissue-mimicking calibration phantom revealed no significant difference between the phantom data in the patients and those in the control subjects as individual groups. For this purpose, a significant difference was defined as $P < .05$. When all anatomic regions were considered together by using the GEE method, 9 of 45 textural features showed statistically significant differences between the patient population and the control group ($P < .04$). Table 3 lists the mean values for both populations (averaged over all anatomic locations) that were significantly different and the appropriate standard error from the GEE analysis for comparing the difference of the means. Figure 4 lists the mean gray levels by anatomic location for the 2 populations. The logistic regression resulted in a combined mean gray level from the cerebellum and the posterior cerebral artery distributions for the most significant difference between the patients and the control subjects. The combined mean gray level (cerebellum and right and left posterior cerebral artery distribution) for patients was 55.1; for control subjects, the value was 41.1 (SE = 4.4, $P = .0021$).

The higher the combined mean gray level (cerebellum and right and left posterior cerebral artery distribution), the more likely the infant was to have suffered a clinical hypoxic episode with resultant brain changes. Figure 5 shows the combined mean gray level for these three anatomic sites versus age for both populations. Fig-

TABLE 3: Mean values of statistically significant textural features for healthy infants and patient population

Feature	Control Subjects (n = 16)	Patients (n = 9)	Standard Error	*P* Value
Mean gray level	46.804	56.317	4.172	.02
Skewness	0.616	0.446	0.066	.02
10th percentile gray levels	15.723	22.449	2.839	.02
90th percentile gray levels	81.682	92.551	4.989	.03
Entropy, east-west, four pixels	7.402	7.516	0.055	.04
Contrast east-west, four pixels	285.836	336.857	18.39	.006
Correlation east-west, four pixels	0.742	0.715	0.012	.02
Correlation north-south, two pixels	0.600	0.618	0.008	.02
Correlation north-south, four pixels	0.308	0.325	0.011	.04

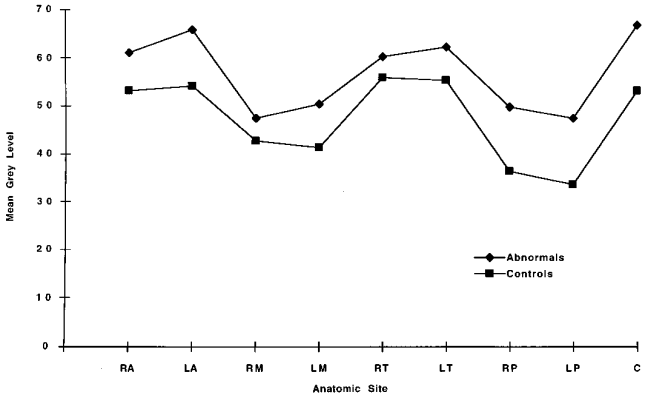

Fig 4. Mean gray levels by anatomic site for patient and control populations. *RA* indicates right anterior; *LA*, left anterior; *RM*, right middle; and *LM*, left middle cerebral artery distributions; *RT*, right thalamus; *LT*, left thalamus; *RP*, right posterior and *LP*, left posterior cerebral artery distributions; and *C*, cerebellum.

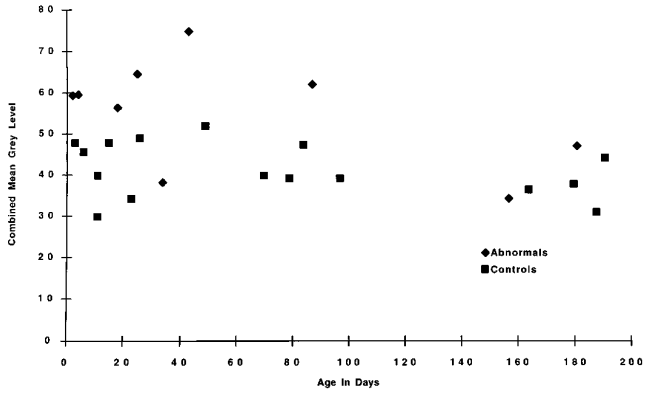

Fig 5. Combined mean gray level for the cerebellum and the right and left posterior cerebral artery distributions expressed as an average value per patient versus patient age.

ure 6 shows the combined mean gray level for the three sites versus the time after insult for the patient group.

Textural measurements obtained from fractal analysis (n = 5), the run-length histogram (n = 8), and gradient analysis (n = 5) failed to show differences between the two populations.

Discussion

Cross-sectional imaging plays an important role in the detection and evaluation of clinical hypoxia. Previous investigators have indicated that neurosonography is capable of detecting increased echogenicity, convolutional effacement, and obliteration of extraaxial fluid spaces after an episode of clinical hypoxia (2). The portability of sonographic equipment is unparalleled. Despite these studies, computed to-

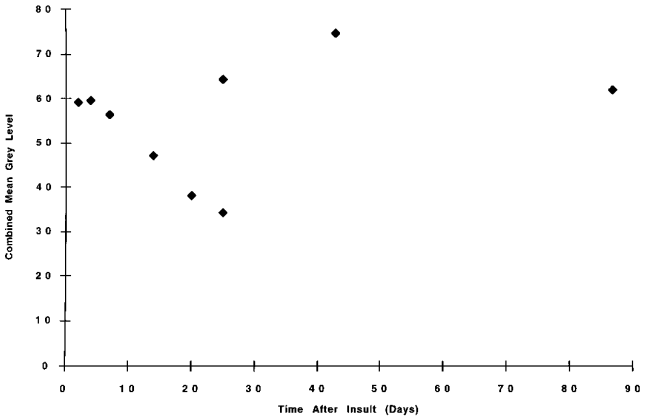

Fig 6. Combined mean gray level for the cerebellum and both posterior cerebral artery distributions expressed as an average value per patient versus time after insult in days.

mography remains the imaging technique of choice at most institutions for the evaluation of hypoxic/ischemic encephalopathy, and is preferred over sonography by many authors (10). Such preference is often dictated by technical variability among sonographic equipment and by interobserver variability in the detection/evaluation of sonographic features. Methods that quantitate sonographic textural features may potentially overcome the difficulty in identifying subtle and/or diffuse changes in echogenicity.

Several textural features in the patients with clinical hypoxia are clearly different from those of healthy infants in this small group of subjects. Four of the textural features demonstrating statistically significant differences were first-order gray-level statistics: mean gray level, skewness of the gray-level distribution, and the 10th and 90th percentile gray levels. These features were all elevated in the patient group, indicating that the lowest 10% of pixel intensities, the mean pixel intensities, and the highest 10% of pixel intensities were greater in the infants with brain injury (Figs 1, 2, and 7). This corresponds to the qualitative finding of increased echogenicity seen on sonograms in approximately 50% of patients with hypoxic/anoxic brain injury (2). Note that the abnormal values parallel the regional distribution of normal values with respect to each anatomic area (Fig 4). This may explain why it is difficult to discern the difference between normal and abnormal echogenicity with the human eye.

The other five features that exhibited a statistically significant difference between the two

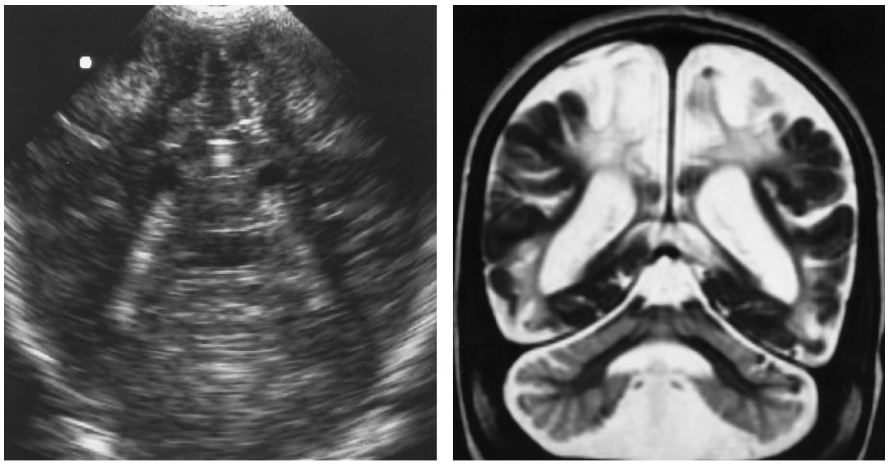

Fig 7. Injury to posterior cerebral artery distributions and cerebellum.

A, Coronal neurosonogram obtained through the occipital lobes and cerebellum of a 6-month-old infant 14 days after an episode of acute status epilepticus. Note increased echogenicity especially evident in the parietooccipital regions. There is coarsening of the echotexture throughout the occipital lobes and cerebellum. This patient's mean gray level was 52.10 and combined mean gray level (cerebellum and right and left posterior cerebral artery distribution) was 47.08.

B, Coronal fast spin-echo magnetic resonance image (2500/119) obtained 2 years later shows profound cortical loss throughout the occipital lobes and cerebellum. This patient had spastic quadriparesis and cortical blindness.

populations were second-order gray-level statistics derived from the gray level co-occurrence matrix (3). Contrast and entropy were significantly elevated in the patient population. Frequent large differences in gray levels increase contrast. Entropy is a measure of the uniformity or lack thereof within the matrix, which increases with increasing coarseness of the ROI. Correlation measures the linearity of the relationship of the gray levels in distance-related pixels in a variety of vector directions. This feature was elevated in the patient population in the vertical direction and decreased in the horizontal direction. These features may correspond to the qualitative detection of inhomogeneity or coarseness of the echotexture by the radiologist.

Our data show the greatest differences in textural features between the two populations in the cerebellum and posterior cerebral artery distributions (Fig 7). These anatomic sites are known to be preferentially affected in association with several patterns of intrapartum and neonatal asphyxia, such as selective neuronal necrosis and parasagittal cerebral injury (11, 12). We know of no published data to indicate which parts of the brain are more prone to show changes in echogenicity in response to hypoxia. Just as magnetic resonance imaging is superior for detecting abnormalities of the basal ganglia in patients with hypoxia, sonography may be more sensitive to the changes occurring in the posterior regions. We postulate that this may be due to the decreased attenuation of the brain in patients with clinical hypoxia, which would result in an increase in the gray level of the pixel intensities in the posterior regions, since the ultrasound beam is attenuated as it travels to and returns from these areas farthest from the transducer.

This pilot project begins to explain sonographic differences between normal and injured brain and further highlights the need for reproducible machine settings on sonographic equipment. Table 1 demonstrates the variability in the settings of one sonographic machine in a single laboratory. Even more variability occurs when images from different machines or different laboratories are compared. Calibration on the current generation of sonographic equipment is difficult owing to the number of dials and toggles that do not give the user numeric output. When the sonographic units become easier to calibrate, then quantitative measurements from studies such as this will be easier to reproduce with different machines and in different laboratories. Independent consoles allowing the radiologist to measure sonographic data much like one measures Hounsfield units would then be a practical method of implementing quantitative sonography in the clinical setting.

In conclusion, our pilot project confirms that quantitative sonographic textural features analysis is useful in differentiating healthy infants from those with clinical hypoxia. Measuring the average mean gray level in the cerebellum and in both posterior cerebral artery distributions yielded a combined value that showed the greatest differences between the two patient populations. The brain is an ideal organ for

quantitative sonographic research because of the stable blood supply and the relatively small amount of variability in the intervening tissues of the anterior fontanelle. Further laboratory experiments to measure directly the sonographic attenuation and speed of sound in acutely injured brain would be necessary to prove the explanations we hypothesize.

Acknowledgments

We gratefully acknowledge access to the digital output of the ultrasound machine from Advanced Technology Laboratories, Inc; the technical assistance of T. Adams, K. Dunn, M. Gramke, L. Muench, S. Shellenbach, T. Vogelsang, G. Berg, S. J. Cho, and C. Ferguson in data collection; and the secretarial assistance of S. Kroeger.

References

1. Stark JE, Seibert JJ. Cerebral artery Doppler ultrasonography for prediction of outcome after perinatal asphyxia. *J Ultrasound Med* 1994;13:595–600
2. Babcock D, Ball W. Postasphyxial encephalopathy in full-term infants: ultrasound diagnosis. *Radiology* 1983;148:417–423
3. Raeth U, Schlaps D, Limberg B, et al. Diagnostic accuracy of computerized B-scan texture analysis and conventional ultrasonography in diffuse parenchymal and malignant liver disease. *J Clin Ultrasound* 1985;13:87–99
4. Haberkorn U, Zuna L, Lorenz A, et al. Echographic tissue characterization in diffuse parenchymal liver disease: correlation of image structure with histology. *Ultrason Imaging* 1990;12:155–170
5. Chen CC, Laponte JS, Fox MD. Fractal feature analysis and classification in medical imaging. *IEEE Trans Med Imaging* 1989;8: 133–141
6. Allison JW, Barr LL, Massoth RJ, et al. Understanding the process of quantitative ultrasonic tissue characterization. *Radiographics* 1994;14:1099–1108
7. Mandelbrot BB. *The Fractal Geometry of Nature.* New York, NY: Freeman; 1983:14–19
8. Zeger S, Liang L. Longitudinal data analysis for discrete and continuous outcomes. *Biometrics* 1986;42:121–130
9. Hosmer DW, Lemeshow S. *Applied Logistic Regression.* New York, NY: John Wiley & Sons; 1989:25–27, 32–33
10. Kolawole TM, Patel PJ, Mahdi AJ. Computed tomographic (CT) scans in cerebral palsy (CP). *Pediatr Radiol* 1989;20:23
11. Low JA, Robertson DM, Simpson LL. Temporal relationships of neuropathologic conditions cause by perinatal asphyxia. *Am J Obstet Gynecol* 1989;160:608–614
12. Hill A, Volpe JJ. Hypoxic-ischemic brain injury in the newborn. *Semin Perinatol* 1982;6:25–40